**ORIGINAL PAPERS**

# 4,4′-Dimethylazobenzene as a chemical actinometer

Lorenzo Casimiro[1] · Leonardo Andreoni[2,3] · Jessica Groppi[3] · Alberto Credi[3,4] · Rémi Métivier[1] · Serena Silvi[2,3]

## Abstract
Chemical actinometers are a useful tool in photochemistry, which allows to measure the photon flux of a light source to carry out quantitative analysis on photoreactions. The most commonly employed actinometers so far show minor drawbacks, such as difficult data treatment, parasite reactions, low stability or impossible reset. We propose herewith the use of 4,4′-dimethylazobenzene as a chemical actinometer. This compound undergoes a clean and efficient *E/Z* isomerization, approaching total conversion upon irradiation at 365 nm. Thanks to its properties, it can be used to determine the photon flux in the UV–visible region, with simple experimental methods and data treatment, and with the possibility to be reused after photochemical or thermal reset.

**Graphical abstract**
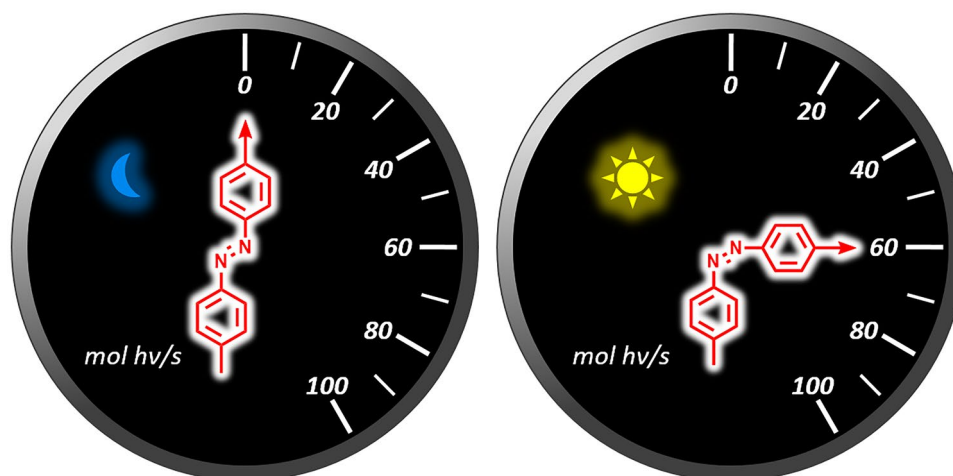
✉ Lorenzo Casimiro
    lorenzo.casimiro@ens-paris-saclay.fr

✉ Serena Silvi
    serena.silvi@unibo.it

1   Université Paris-Saclay, ENS Paris-Saclay, CNRS, PPSM-UMR 8531, 91190 Gif-sur-Yvette, France

2   Dipartimento di Chimica "G. Ciamician", Università di Bologna, 40126 Bologna, Italy

3   CLAN-Center for Light Activated Nanostructures, Istituto ISOF-CNR, via Gobetti 101, 40129 Bologna, Italy

4   Dipartimento di Chimica Industriale "Toso Montanari", Università di Bologna, 40136 Bologna, Italy

## 1 Introduction

The measurement of incident photon fluxes represents a crucial point for the analysis of photoreactions. For this purpose, chemical actinometers [1–5], i.e., chemical species that undergo a photoreaction with known quantum yield, are currently widely used both for UV and visible light. Although they usually provide reliable results by simple measurement and data treatment procedures, chemical actinometers must satisfy several requirements: the system must be simple and well characterized, thermally stable and easy to synthesize or, preferably, commercially available; the photoproduct should be inert; the quantum yields values must be known

with high precision, reproducible and ideally independent on the irradiation wavelength, the temperature, the concentration and/or the presence of oxygen; the system should have a high absorption coefficient at the irradiation wavelength; finally, the analytical procedure must be easy and rapid, ideally a simple absorption measurement [1].

Among the numerous actinometers reported so far, the most employed ones are the potassium ferrioxalate—or *Hatchard–Parker actinometer* (250–500 nm) [6–13], the *Aberchrome 540* (310–375 nm and 435–535 nm) [14–24], and the potassium reineckate—or *Reinecke's salt* (316–750 nm) [4, 25–28]. However, despite their well consolidated and good performances, none of these fulfills all the above-mentioned requirements. Azobenzene [29–31] has also been used as a chemical actinometer [1, 32–41]. His clean and reversible *E/Z* photoisomerization has been extensively studied in a wide range of solvents [29, 31] and the photoisomerization quantum yield (*Φ*) values have been accurately determined [42, 43]. However, despite being commercially available, this compound has been classified as a suspect carcinogenic agent [44]. Moreover, the absorption coefficient of azobenzene at 365 nm, the most intense line of medium-pressure mercury lamps, is really poor and this feature limits its use as actinometer at this particular wavelength. Finally, the data treatment is not easy and the procedure is limited to the sole UV range.

Herein we report the complete photochemical characterization of an azobenzene derivative, the 4,4′-dimethylazobenzene (DMAB, Fig. 1). This compound can be easily synthesized, and it displays a clean *E–Z* isomerization, with a slow thermal back process and an excellent fatigue resistance. Interestingly, thanks to its optical properties, the photoconversion approaches the unity under irradiation at 365 nm. Therefore, we suggest the employment of such compound as a chemical actinometer, its properties allowing an easy manipulation and reliable results.

## 2 Results and discussion

DMAB (Fig. 1) is commercially available. However, it can be synthesized in good yields, according to well-known procedures [45, 46]. In the present study, we synthesized the
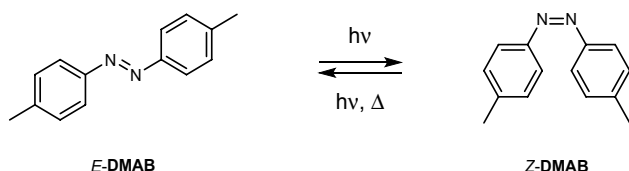
compounds according to the procedure reported in the SI (Section 1).

### 2.1 UV–vis characterization and determination of the spectrum of the *Z* isomer

Absorption spectra were recorded in air-equilibrated acetonitrile (MeCN) solutions at room temperature. The absorption spectrum of *E*-DMAB (Fig. 2, figure S1) is in line with those already reported in the same or different solvents [44, 47–57], and shows the two peculiar bands of azobenzene derivatives: an intense π–π* band, centered at 333 nm, with an absorption coefficient (*ε*) value of 27,400 $M^{-1}$ $cm^{-1}$, and a weaker n–π* band, centered at 440 nm, with an *ε* of 800 $M^{-1}$ $cm^{-1}$. These two bands are non-structured and well resolved as it usually occurs in azobenzene-type compounds [29, 31, 58]. A third band, with an *ε* of 15,000 $M^{-1}$ $cm^{-1}$ at 235 nm, can be ascribed to the $S_0$–$S_3$ transition. With respect to *E*-DMAB, the absorption spectrum of *Z*-DMAB (Fig. 2, figure S1) [47] is characterized by a less intense and blueshifted π–π* band (*ε* = 6000 $M^{-1}$ $cm^{-1}$ at 289 nm) and a more intense n–π* band (*ε* = 1800 $M^{-1}$ $cm^{-1}$ at 436 nm). Conversely, the $S_0$–$S_3$ band is redshifted of 11 nm, with an *ε* of 12,100 $M^{-1}$ $cm^{-1}$ at 246 nm.

Upon irradiation with UV or visible light, DMAB underwent *E–Z* photoisomerization on the central azo bond [54–56, 59]: the absorbance of the π–π* band deeply decreased, and the one of the n-π* increased, until a photostationary state (*PSS*) was achieved (Fig. 3).

Since the absorption spectra of the two isomers are overlapped over the whole UV–vis spectral range, the pure *Z* isomer cannot be obtained, albeit irradiation at 365 nm affords an almost complete photoconversion (*vide infra*). Photostationary states (see Table 1, figure S2), are more shifted
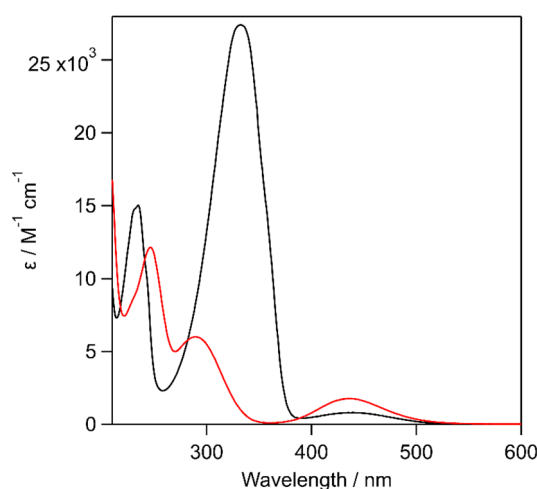


**Fig. 1** Structure and photoisomerization reactions of DMAB



**Fig. 2** Absorption spectra of the *E* (black line) and *Z* (red line) isomers of DMAB in MeCN
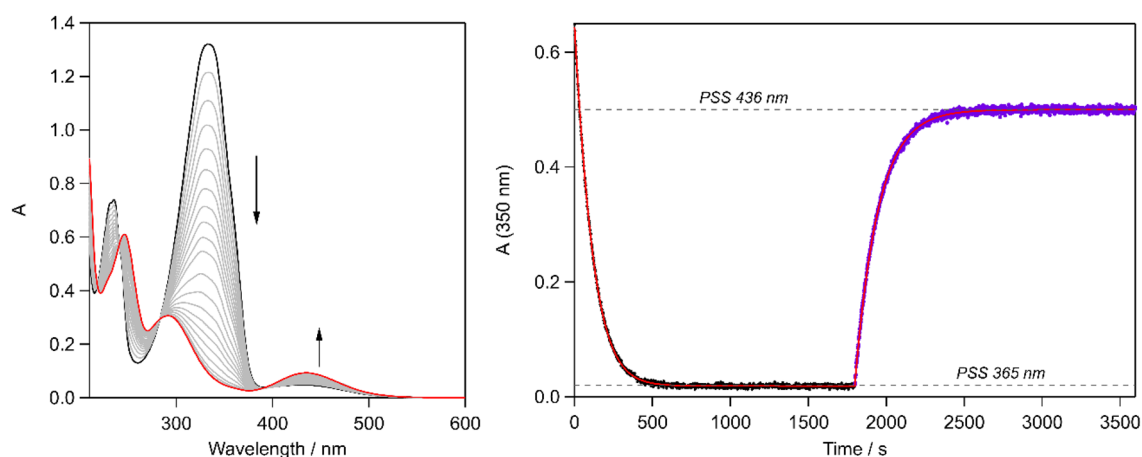
**Fig. 3** Left: Absorption variation of a $4.7 \times 10^{-5}$ M solution of DMAB upon irradiation at 365 nm; right: consecutive irradiations at 365 nm (black dots) and at 436 nm (purple dots) of a $3.0 \times 10^{-5}$ M solution of DMAB in MeCN, with fitting (red lines, see text for details)

**Table 1** Average values of absorption coefficients ($\varepsilon$), photoisomerization quantum yields ($\Phi_{EZ}$ and $\Phi_{ZE}$), and photoconversion extents ($\alpha$) at the photostationary states of DMAB for the main lines of a medium-pressure mercury lamp

| $\lambda_{irr}$/nm | $\varepsilon_E$/M$^{-1}$ cm$^{-1}$ | $\varepsilon_Z$/M$^{-1}$ cm$^{-1}$ | $\Phi_{EZ} \pm \sigma$ | $\Phi_{ZE} \pm \sigma$ | Number of measures | $\alpha$ |
|---|---|---|---|---|---|---|
| 254 | 2493 | 10,038 | $0.20 \pm 0.01$ | $0.43 \pm 0.01$ | 6 | 0.11 |
| 297/302 | 14,284[a] | 5272[a] | $0.18 \pm 0.01$ | $0.39 \pm 0.01$ | 7 | 0.53 |
| 313 | 20,749 | 3640 | $0.17 \pm 0.01$ | $0.42 \pm 0.02$ | 8 | 0.71 |
| 334 | 27,385 | 850 | $0.20 \pm 0.01$ | $0.43 \pm 0.02$ | 6 | 0.94 |
| 365 | 8311 | 101 | $0.18 \pm 0.01$ | $0.34 \pm 0.06$ | 8 | 0.97 |
| 405 | 529 | 978 | $0.29 \pm 0.01$ | $0.52 \pm 0.01$ | 7 | 0.24 |
| 436 | 786 | 1766 | $0.30 \pm 0.01$ | $0.45 \pm 0.01$ | 8 | 0.23 |

[a]Average of the absorption coefficients values at the two wavelengths, weighted by the contribution of each mercury line (38% at 297 nm, 62% at 302 nm)

toward the *Z* isomer upon irradiation on the π–π* band, up to a maximum of 0.97 at 365 nm. Conversely, irradiation on the n–π* or S$_3$ bands leads to PSSs less rich in *Z* isomer, with photoconversion extents up to a maximum of 0.24 at 405 nm [48, 49, 54, 57, 59]. Interestingly, the PSS obtained with 254 nm light has a content of *Z* isomer as low as 11%; therefore irradiation at this wavelength could be considered as a way to speed up the recovery of the *E* form. However, the fatigue resistance is likely to be lower under irradiation with more energetic light (such as 254 nm); therefore we encourage to recover the *E* form thermally.

To test the fatigue resistance of DMAB, we performed alternated irradiation at 365 nm and 436 nm. The compounds switched efficiently between the two photostationary states, without any evidence of degradation after more than 100 cycles (figure S3).

When left in the dark, previously irradiated solutions showed a thermally accessible back isomerization process, and the spectrum of the *E* isomer was recovered in several days (figure S4, SI). The rate constant ($k_\Delta$) is $1.6 \times 10^{-6}$ s$^{-1}$, which suggests that the thermal back isomerization is substantially negligible in the typical experimental timescales (from few minutes to one day).

Despite the pure *Z* isomer could not be produced photochemically [43, 47], we extracted its absorption spectrum by two spectroscopic methods, which gave comparable results. The first method, reported by Thulstrup, Eggers and Michl (hence the acronym *TEM*) [60, 61], consists in subtracting from the second derivative of the spectrum of the *E* isomer, the second derivative of the absorption spectrum of a PSS multiplied by an arbitrary value of α. Since the π–π* band of *E*-DMAB has a vibrational structure—albeit low— and *Z*-DMAB has none, the right value of *α* can be found once the subtraction leads to the complete disappearance of the vibrational structure. In our case, we applied the *TEM* method to the PSS obtained upon irradiation at 365 nm, obtaining $\alpha = 97\%$.

The second method to obtain the photoconversion and the absorption coefficient of the *Z* isomer, reported by Fischer [62], was applied using the two photostationary states produced under irradiation at 334 nm and 365 nm. The spectrum obtained through this protocol, reported in Fig. 2,

has been used to calculate the remainder photochemical parameters.

## 2.2 Photokinetic considerations and photoisomerization quantum yields determination

The photoreaction of a T-type photochrome, whose two forms are both photoactive, is described by the following photokinetic equation [2, 63, 64]

$$\frac{\mathrm{d}[E]}{\mathrm{d}t} = -\frac{\mathrm{d}[Z]}{\mathrm{d}t} = -\frac{\Phi_{EZ} \cdot q_0}{V} \cdot \frac{\varepsilon_{E,\lambda_i} \cdot [E] \cdot f}{\left(\varepsilon_{E,\lambda_i} \cdot [E] + \varepsilon_{Z,\lambda_i} \cdot [Z]\right)}$$
$$+ \frac{\Phi_{ZE} \cdot q_0}{V} \cdot \frac{\varepsilon_{Z,\lambda_i} \cdot [Z] \cdot f}{\left(\varepsilon_{E,\lambda_i} \cdot [E] + \varepsilon_{Z,\lambda_i} \cdot [Z]\right)} + k_\Delta \cdot [Z] \quad (1)$$

In this equation $\Phi_{EZ}$ and $\Phi_{ZE}$ are the quantum yields of $E–Z$ and $Z–E$ isomerization, respectively, $q_0$ is the incident photon flux, $\varepsilon_{\lambda_i}$ are the absorption coefficients of the $E$- and $Z$ isomers at the irradiation wavelength $\lambda_i$, $f$ is the fraction of light absorbed by the sample, calculated from the absorbance of the mixture at the irradiation wavelength $\lambda_i$, according to equation

$$f = 1 - 10^{-A_{\lambda_i}} = 1 - 10^{-\left(\varepsilon_{E,\lambda_i} \cdot [E] + \varepsilon_{Z,\lambda_i} \cdot [Z]\right)} \quad (2)$$

which, in Eq. (1), is multiplied by the contribution of each isomer to the absorbed light, and $k_\Delta[Z]$ is the contribution of the thermal process (the optical path of the cuvette is considered 1 cm and henceforth it will be omitted for clarity). It is worth to remark that both the concentrations and the absorbances are time-dependent and prevent the analytical solution of the differential equation.

We measured the photoisomerization quantum yields of DMAB through an apparatus that allowed us to simultaneously irradiate the solution and record the absorption spectra over time. The solution was carefully stirred throughout the whole irradiation, to avoid measurements on non-homogeneous points of the solution. The incident photon flux $q_0$ was measured with a photodiode. We then fitted the time-dependent absorption evolution (see Fig. 3) according to the differential equation (1).

The photoisomerization quantum yields, measured for the main lines of a medium-pressure mercury lamp, are reported in Table 1.

It is worth to remark that, in the fitting process, the most reliable result is the one of the forward reaction, whereas the backward is affected by a larger error. Therefore, in the case of 254 nm, 405 nm and 436 nm, whose photostationary states are shifted to the $E$ form, we minimized the error

on the $\Phi_{ZE}$ values (to be used for actinometry, *vide infra*), conducting the photokinetic experiments on solutions previously irradiated at 365 nm or 334 nm.

The resulting quantum yield values are in line with similar compounds previously reported in literature [48, 49, 57]. Upon irradiation on the π–π* band, the $E$-to-$Z$ quantum yield is around 0.18 and the $Z$-to-$E$ quantum yield is around 0.40. Both these values are slightly larger upon irradiation on the n-π* band.

## 3 Actinometry protocol

### 3.1 Data treatment and recommendations

The application of DMAB as an actinometer requires a faster and easier procedure than a photokinetic fitting. Since the $Z–E$ thermal process is slow enough to be neglected in the experimental timescales, as long as the concentration of the photoproduct is negligible and it does not contribute significantly to the absorbance, the sole process occurring is the $E–Z$ photoisomerization and the Eq. (1) reduces to [2, 63]

$$\frac{\mathrm{d}[E]}{\mathrm{d}t} = -\frac{\Phi_{EZ} \cdot q_0 \cdot f}{V} \quad (3)$$

As a general rule, we assume that the absorbance of the photoproduct is negligible as long as it is at least 20 times lower than the absorbance of the reactant, i.e., the following condition is satisfied [64]

$$[E] \cdot \varepsilon_E \geq 20 \cdot [Z] \cdot \varepsilon_Z \quad (4)$$

For short irradiation time intervals and for small variations of absorbance, it can be assumed that $f$ is equal to the average value

$$f_{\mathrm{ave}} = \frac{f_0 + f_1}{2} \quad (5)$$

where $f_0$ and $f_1$ are the fractions of light absorbed before and after the irradiation. In these conditions, we can use the Eq. (3) in its discrete form (6)

$$\Delta[E] = -\frac{\Phi_{EZ} \cdot q_0}{V} \cdot f_{\mathrm{ave}} \cdot \Delta t_{\mathrm{irr}} \quad (6)$$

where $\Delta t_{\mathrm{irr}}$ is the time interval of short irradiation. The concentration can be related to the absorbance at a chosen wavelength $\lambda_x$ through the difference of the absorption coefficients at that wavelength, thus

$$\Delta[E] = \frac{\Delta A_{\lambda_x}}{\Delta \varepsilon_{\lambda_x}} = \left(\frac{A_t - A_0}{\varepsilon^Z - \varepsilon^E}\right)_{\lambda_x} \quad (7)$$

The combination of equations (6) and (7), rearranged with respect to time 0, eventually provides

$$A = A_0 - \left( \frac{q_0 \cdot \Phi_{EZ} \cdot \Delta\varepsilon_{\lambda_x}}{V} \right) (f_{ave} \cdot t) \qquad (8)$$

If the absorbance at the irradiation wavelength remains above 3 throughout the whole irradiation time (total absorption regime), the fraction of absorbed light equals 1 and the equation simplifies in [2, 63, 64]

$$A = A_0 - \left( \frac{q_0 \cdot \Phi_{EZ} \cdot \Delta\varepsilon_{\lambda_x}}{V} \right) t \qquad (9)$$

In both equations (8) and (9) the absorbance variation in function of the time of irradiation is a straight line, having the absorbance value before irradiation—i.e., at time 0—as intercept and containing the photon flux in the slope. Therefore, $q_0$ can be calculated from the slope $m$ obtained by a linear fitting of the absorbance over ($f \cdot t$) or $t$, respectively.

$$q_0 = \frac{m \cdot V}{\Phi_{EZ} \cdot \Delta\varepsilon_{\lambda_x}} \qquad (10)$$

We propose the following procedures in two absorbance regimes, successfully tested in our laboratory with the ferrioxalate actinometer (see section 4 of the SI for details).

We recommend to work in total absorption regime when possible, as the data treatment is the easiest. Using a solution with concentration above $5 \times 10^{-4}$ M is suggested for the range 302-365 nm (procedure A). However, keeping a total absorption regime at the irradiation wavelengths 254 nm, 405 nm, 436 nm throughout the whole measurement would mean that only a spare region of the spectrum is at suitable absorbance values to obtain a reliable measurement. Therefore, in these cases, we recommend to use more diluted solutions and calculate the average fraction of absorbed light for each irradiation step (procedure B). In any case, diluted solutions can be used for all the irradiation wavelengths, provided that average $f$ is taken into account.

To ensure that the concentration of the photoproduct is negligible and the absorbance does not fall below 3 (when working in total absorption regime), we recommend also to keep the photoconversion extent below the 10%.

The $E$ form can be recovered thermally, by leaving the compound at room temperature for at least one month before reuse. To speed up the procedure, we suggest to illuminate it in the visible, where the photostationary states reach an $E{:}Z$ ratio of around 20:80, or at 254 nm, where this ratio is 11:89, and leave the reaction complete thermally.

(A) **Actinometric procedure for total absorption regime – range 302 nm – 365 nm**

1. Place 3 mL of a DMAB solution in MeCN with a concentration not lower than $5 \times 10^{-4}$ M in a 1 cm pathlength cuvette with a suitable magnetic stirrer
2. Record the absorption spectrum before irradiation
3. Irradiate the sample for a known time interval, under continuous stirring
4. Record the absorption spectrum
5. Repeat points (3) and (4) for at least other 2 times on the same solution, checking that the 10% of photoconversion is not exceeded
6. Plot the absorbance values at 440 nm vs time
7. Fit according to a linear equation

$$y_0 - mx$$

Which physically corresponds to

$$A = A_0 - \left( \frac{q_0 \cdot \Phi_{EZ} \cdot \Delta\varepsilon_{\lambda_x}}{V} \right) t$$

Calculate $q_0$ from the obtained slope $m$

$$q_0 = \frac{m \cdot V}{\Phi_{EZ} \cdot \Delta\varepsilon_{\lambda_x}}$$

For a further simplification of the data treatment, the constant values $V$, $\Phi_{EZ}$ and $\Delta\varepsilon$ at 440 nm ($\varepsilon_E = 798$ M$^{-1}$ cm$^{-1}$, $\varepsilon_Z = 1747$ M$^{-1}$ cm$^{-1}$) can be gathered in a parameter $X$, listed in Table 2, thus:

$q_0 = m \cdot X$.

(B) **Actinometric procedure for intermediate absorption regime—range 254–436 nm**

1. Place 3 mL of a solution of DMAB in MeCN, with a concentration comprised between 2 and $5 \times 10^{-4}$ M, in a 1 cm pathlength cuvette with a suitable magnetic stirrer
2. Record the absorption spectrum before irradiation
2a. Only for irradiations at 254 nm, 405 nm and 436 nm: Irradiate the sample at 365 nm to reach the photostationary state and record the absorption spectrum

**Table 2** $X$ factor for the actinometric procedure in total absorption regime

| $\lambda_{irr}$/nm | $X/10^{-5}$ mol |
|---|---|
| 297/302 | 1.76 |
| 313 | 1.86 |
| 334 | 1.58 |
| 365 | 1.76 |

3. Irradiate the sample at the desired wavelength for a known time interval, under continuous stirring
4. Record the absorption spectrum
5. Repeat points (3) and (4) for at least other 2 times on the same solution, checking that the 10% of photoconversion is not exceeded
6. Plot the absorbance values at 333 nm vs the total irradiation time multiplied for the value of $f_{ave}$ for the corresponding irradiation step
7. Fit according to a linear equation

$$y = y_0 - mx$$

Which physically corresponds to

$$A = A_0 - \left( \frac{q_0 \cdot \Phi_i \cdot \Delta\varepsilon_{\lambda_x}}{V} \right)(f_{ave} \cdot t)$$

where $\Phi_i$ is $\Phi_{ZE}$ when irradiating at 254 nm, 405 nm and 436 nm, $\Phi_{EZ}$ at the other wavelengths.

Calculate $q_0$ from the obtained slope m

$$q_0 = \frac{m \cdot V}{\Phi_i \cdot \Delta\varepsilon_{\lambda_x}}$$

For a further simplification of the data treatment, the constant values $V$, $\Phi_i$ and $\Delta\varepsilon$ at 333 nm ($\varepsilon_E = 27{,}421\ M^{-1}\ cm^{-1}$, $\varepsilon_Z = 933\ M^{-1}\ cm^{-1}$) can be gathered in a parameter $Y$, listed in Table 3, thus:

$$q_0 = m \cdot Y$$

# 4 Conclusions

We reported the photochemical characterization of 4,4'-dimethylazobenzene (DMAB), which we suggest to use as a chemical actinometer on account of the advantages listed below:

- Availability: DMAB is commercially available; nevertheless, it can be synthesized easily and on large scales, with excellent reaction yields. Other actinometers commonly used nowadays are not commercial and require synthetic efforts or purification procedures: Aberchrome is no longer commercially available and must be synthesized; potassium ferrioxalate and Reinecke's salt must be recrystallized to obtain a suitable purity [25, 27]; azobenzene is commercially available, but known to be carcinogenic and its use should be discouraged.

- Experimental procedure: E-DMAB isomer does not undergo thermal reactions or degradations, thus a blank is not required (as for Reinecke's salt [26] and ferrioxalate [7]). The absorbance recording does not need any dilution (as for Reinecke's salt) [25, 27] or addition of reactants (as o-phenanthroline for ferrioxalate or Fe(NO₃)₃ for Reinecke's salt). Therefore, the manual errors arising from the procedure are largely minimized using DMAB.

- Stability: E-DMAB is stable in solutions kept in the dark; other commonly used actinometers, such as ferrioxalate and Reinecke's salt [7, 26], can give thermally the same reaction used for actinometry. Aberchrome solutions cannot be reused after bleaching, since a parasite Z isomer of the open form is accumulated and interferes with the photoreaction [18, 19]. Moreover, in case of DMAB, a minor increase in concentration due to the volatility of MeCN can be disregarded, as the data treatment does not require a known concentration value.

- Reset: The same solution can be used more than once, by resetting the Z form to the E, either photochemically (at 254 nm or in the visible) or thermally, by leaving the compound at room temperature for 1 month. The excellent fatigue resistance allows to perform measurements on the same solutions up to at least 50 times.

- Data treatment: The thermal isomerization is negligible, and, at low photoconversion extent, the absorption contribution of the Z isomer can be neglected too. Consequently, the quantum yield equation can be reconducted to a linear relationship.

- Total absorption regime: The absorption coefficient at 365 nm is larger with respect to azobenzene [55], because of the redshift of the π-π* band. If the absorbance at this wavelength is larger than 3, there is still a portion of spectrum below 1 that can be used for the data treatment. This allows to use the compound in total absorption regime up to 365 nm.

- Visible region: The PSSs in the visible (405 nm, 436 nm) are less rich in Z isomer, leading to a lower signal if the irradiation is performed starting from the pure E isomer. However, since the PSS at 365 nm is close to the pure Z isomer, the actinometry in the visible can be carried out starting from this PSS, with a

**Table 3** $Y$ factor for the actinometric procedure in intermediate absorption regime

| $\lambda_{irr}/nm$ | $Y/10^{-7}$ mol |
|---|---|
| 254 | 2.63 |
| 297/302 | − 6.29 |
| 313 | − 6.66 |
| 334 | − 5.66 |
| 365 | − 6.29 |
| 405 | 2.18 |
| 436 | 2.52 |

larger absorption variation and with a data treatment identical to the *E-Z* isomerization.

## 5 Methods

Steady-state spectroscopic measurements were performed on air-equilibrated solutions at room temperature in spectroscopic grade (Uvasol, Carlo Erba) acetonitrile (MeCN), placed in 1 cm pathlength quartz cuvettes. Absorption spectra were recorded on a Cary100 spectrophotometer from Agilent Technologies.

Photoisomerization reactions were induced by a Hamamatsu Hg/Xe Lamp Lightningcure LC8 or by a Helios Quartz medium-pressure Hg Lamp. The desired Hg emission line was selected by means of an appropriate interference filter (Semrock filters: FF01-254/8-25, FF01-292/27-25 + FF01-320/40-25, FF01-315/15-25 + FF01-320/40-25, FF01-335/7-25, FF01-370/10-25, FF01-406/15-25, FF01-438/24-25) or a monochromator SPEX 1681. The lamp power was measured by means of an Ophir PD300-UV photodiode. NIR contribution was measured and subtracted from the total value. Photoisomerization quantum yields and fatigue resistances were determined using a home-made setup, which collects absorption spectra at high rates, under continuous irradiation. A Xenon lamp (75 W) was employed as a probing light and a Hg/Xe lamp, placed at 90° with respect to the incident beam, was used to photoisomerize the sample, placed in a cuvette and thoroughly stirred. Spectra were recorded every 0.1 seconds, with a spectrograph equipped with a CCD camera (Roper Scientific and Princeton Instruments, respectively). Photokinetic profiles were then fitted using a numerical iterative fitting method implemented in an Igor procedure (Wavemetrics).

Thermal isomerization kinetics measurements were performed on solutions previously irradiated at 365 nm, by monitoring the absorbance variations over time in the dark and at room temperature (298 K). For comparative measurements, potassium ferrioxalate was employed as an actinometer in its "microversion" [2, 8].

**Author contributions** SS and LC conceived the project, LA and JG synthesized the compound, all the authors conducted the experiments, analyzed the results and reviewed the manuscript.

## Declarations

## References

1. Kuhn, H. J., Braslavsky, S. E., & Schmidt, R. (2004). Chemical actinometry (IUPAC technical report). *Pure and Applied Chemistry, 76*, 2105–2146.
2. Montalti, M., Credi, A., Prodi, L., & Gandolfi, M. T. (2006). *Handbook of Photochemistry*. CRC Press.
3. Scaiano, J. C. (2020). *Handbook of Organic Photochemistry*. CRC Press.
4. Braun, A. M., Maurette, M.-T., & Oliveros, E. (1991). *Photochemical Technology*. Wiley.
5. Murov, S. L., Carmichael, I., & Hug, G. L. (1993). *Handbook of Photochemistry* (2nd ed.). Taylor & Francis.
6. Parker, C. A., & Bowen, E. J. (1953). A new sensitive chemical actinometer. I. Some trials with potassium ferrioxalate. *Proceedings of the Royal Society of London Series A, Mathematical and Physical Sciences, 220*, 104–116.
7. Hatchard, C. G., Parker, C. A., & Bowen, E. J. (1956). A new sensitive chemical actinometer—II. Potassium ferrioxalate as a standard chemical actinometer. *Proceedings of the Royal Society of London Series A, Mathematical and Physical Sciences, 235*, 518–536.
8. Fischer, E. (1984). Ferri-oxalate actinometry. *EPA Newsletter, 21*, 33–34.
9. Lee, J., & Seliger, H. H. (1964). Quantum yield of the ferrioxalate actinometer. *The Journal of Chemical Physics, 40*, 519–523.
10. Bowman, W. D., & Demas, J. N. (1976). Ferrioxalate actinometry. A warning on its correct use. *Journal of Physical Chemistry, 80*, 2434–2435.
11. Nicodem, D. E., Cabral, M. L. P. F., & Ferreira, J. C. N. (1977). The use of 0.15 M potassium ferrioxalate as a chemical actinometer. *Molecular Photochemistry, 8*, 213–238.
12. Demas, J. N., Bowman, W. D., Zalewski, E. F., & Velapoldi, R. A. (1981). Determination of the quantum yield of the ferrioxalate actinometer with electrically calibrated radiometers. *Journal of Physical Chemistry, 85*, 2766–2771.
13. Kirk, A. D., & Namasivayam, C. (1983). Errors in ferrioxalate actinometry. *Analytical Chemistry, 55*, 2428–2429.
14. Darcy, P. J., Heller, H. G., Strydom, P. J., & Whittall, J. (1981). Photochromic heterocyclic fulgides. Part 2. Electrocyclic reactions of (E)-α-2,5-dimethyl-3-furylethylidene(alkyl-substituted methylene)succinic anhydrides. *Journal of the Chemical Society, Perkin Transactions, 1*, 202–205. https://doi.org/10.1039/P19810000202

15. Heller, H. G., & Langan, J. R. (1981). Photochromic heterocyclic fulgides. Part 3. The use of (E)-α-(2,5-dimethyl-3-furylethylidene)(isopropylidene)succinic anhydride as a simple convenient chemical actinometer. *Journal of the Chemical Society, Perkin Transactions, 2*, 341–343. https://doi.org/10.1039/P29810000341

16. Rappon, M., & Syvitski, R. T. (1996). Kinetics of photobleaching of Aberchrome 540 in various solvents: Solvent effects. *Journal of Photochemistry and Photobiology, A: Chemistry, 94*, 243–247.

17. Heller, H. G., & Langan, J. R. (1981). A new reusable chemical actinometer. *EPA Newsletter, 13*, 72–73.

18. Yokoyama, Y., Goto, T., Inoue, T., Yokoyama, M., & Kurita, Y. (1988). Fulgides as efficient photochromic compounds. Role of the substituent on furylalkylidene moiety of furylfulgides in the photoreaction. *Chemistry Letter, 17*, 1049–1052.

19. Boule, P., & Pilichowski, J. F. (1993). Comments about the use of Aberchrome™ 540 in chemical actinometry. *Journal of Photochemistry and Photobiology, A: Chemistry, 71*, 51–53.

20. Guo, Z., Wang, G., Tang, Y., & Song, X. (1995). Photokinetic study on the photochromic reaction of Aberchrome 540™: A further comment about the use of Aberchrome 540™ in chemical actinometry. *Journal of Photochemistry and Photobiology, A: Chemistry, 88*, 31–34.

21. Uhlmann, E., & Gauglitz, G. (1996). New aspects in the photokinetics of Aberchrome 540. *Journal of Photochemistry and Photobiology, A: Chemistry, 98*, 45–49.

22. Yokoyama, Y., Hayata, H., Ito, H., & Kurita, Y. (1990). Photochromism of a furylfulgide, 2-[1-(2,5-Dimethyl-3-furyl)ethylidene]-3-isopropylidenesuccinic anhydride in solvents and polymer films. *Bulletin Chemical Society of Japan, 63*, 1607–1610.

23. Deblauwe, V., & Smets, G. (1988). Quantum yields of the photochromic reactions of heterocyclic fulgides and fulgimides. *Die Makromolekulare Chemie, 189*, 2503–2512.

24. Glaze, A. P., Heller, H. G., & Whittall, J. (1992). Photochromic heterocyclic fulgides. Part 7. (E)-Adamantylidene-[1-(2,5-dimethyl-3-furyl)ethylidene]succinic anhydride and derivatives: model photochromic compounds for optical recording media. *Journal of the Chemical Society, Perkin Transactions, 2*, 591–594. https://doi.org/10.1039/P29920000591

25. Wegner, E. E., & Adamson, A. W. (1966). Photochemistry of complex ions. III. Absolute quantum yields for the photolysis of some aqueous chromium(III) complexes chemical actinometry in the long wavelength visible region. *Journal of the American Chemical Society, 88*, 394–404.

26. Adamson, A. W. (1958). Substitution reactions of Reinecke's salt. *Journal of the American Chemical Society, 80*, 3183–3189.

27. Szychliński, J., Bilski, P., Martuszewski, K., & Błażejowski, J. (1989). Complementary study on the use of the potassium Reinecke's salt as a chemical actinometer. *The Analyst, 114*, 739–741.

28. Cornet, J.-F., Marty, A., & Gros, J.-B. (1997). Revised technique for the determination of mean incident light fluxes on photobioreactors. *Biotechnology Progress, 13*, 408–415.

29. Beharry, A. A., & Woolley, G. A. (2011). Azobenzene photoswitches for biomolecules. *Chemical Society Reviews, 40*, 4422–4437.

30. Baroncini, M., Ragazzon, G., Silvi, S., Venturi, M., & Credi, A. (2020). The eternal youth of azobenzene: new photoactive molecular and supramolecular devices. *Pure and Applied Chemistry, 87*, 537–545.

31. Bandara, H. M. D., & Burdette, S. C. (2012). Photoisomerization in different classes of azobenzene. *Chemical Society Reviews, 41*, 1809–1825.

32. Siampiringue, N., Guyot, G., Monti, S., & Bortolus, P. (1987). The cis → trans photoisomerization of azobenzene: An experimental re-examination. *Journal of Photochemistry, 37*, 185–188.

33. Roseau, M., et al. (2021). Azobenzene: A visible-light chemical actinometer for the characterization of fluidic photosystems. *Helvetica Chimica Acta, 104*, e2100071.

34. Rau, H. (1984). Further evidence for rotation in the π, π* and inversion in the n, π* photoisomerization of azobenzenes. *Journal of Photochemistry, 26*, 221–225.

35. Gauglitz, G., & Hubig, S. (1985). Chemical actinometry in the UV by azobenzene in concentrated solution: A convenient method. *Journal of Photochemistry, 30*, 121–125.

36. Gauglitz, G. (2003). Chapter 2—Photophysical, Photochemical and Photokinetic Properties of Photochromic Systems. In H. Dürr, H. B. T.-P. Bouas-Laurent (Eds.), pp. 15–63. Berlin: Elsevier Science. https://doi.org/10.1016/B978-044451322-9/50006-3.

37. Zimmerman, G., Chow, L.-Y., & Paik, U.-J. (1958). The Photochemical Isomerization of Azobenzene1. *Journal of the American Chemical Society, 80*, 3528–3531.

38. Birnbaum, P. P., & Style, D. W. G. (1954). The photo-isomerization of some azobenzene derivatives. *Transactions of the Faraday Society, 50*, 1192–1196.

39. Ronayette, J., Arnaud, R., Lebourgeois, P., & Lemaire, J. (1974). Isomérisation photochimique de l'azobenzène en solution. I. *Canadian Journal of Chemistry, 52*, 1848–1857.

40. Gauglitz, G. (1976). Azobenzene as a convenient actinometer for the determination of quantum yields of photoreactions. *Journal of Photochemistry, 5*, 41–47.

41. Gauglitz, G., & Hubig, S. (1981). Azobenzene as a convenient actinometer: Evaluation values for UV mercury lines and for the N2 laser line. *Journal of Photochemistry, 15*, 255–257.

42. Ladányi, V., et al. (2017). Azobenzene photoisomerization quantum yields in methanol redetermined. *Photochemical &amp; Photobiological Sciences, 16*, 1757–1761.

43. Vetráková, Ľ., et al. (2017). The absorption spectrum of cis-azobenzene. *Photochemical &amp; Photobiological Sciences, 16*, 1749–1756.

44. Mori, Y., NIiwa, T., & Toyoshi, K. (1981). Carcinogenic azo dyes. XVIII. Syntheses of azo dyes related to 3'-hydroxymethyl-4-(dimethylamino) azobenzene, a new potent hepatocarcinogen. *Chemical and Pharmaceutical Bulletin Tokyo, 29*, 1439–1442.

45. Pariyar, G. C., Kundu, T., Mitra, B., Mukherjee, S., & Ghosh, P. (2020). Ethyl lactate: An efficient green mediator for transition metal free synthesis of symmetric and unsymmetric azobenzenes. *ChemistrySelect, 5*, 9781–9786.

46. Selvam, P., Mohapatra, S. K., Sonavane, S. U., & Jayaram, R. V. (2004). Chemo- and regioselective reduction of nitroarenes, carbonyls and azo dyes over nickel-incorporated hexagonal mesoporous aluminophosphate molecular sieves. *Tetrahedron Letters, 45*, 2003–2007.

47. Cook, A. H., Jones, D. G., & Polya, J. B. (1939). cis-Azo-compounds. Part III. Absorption spectra. *Journal of the Chemical Society, 280*, 1315–1320. https://doi.org/10.1039/JR9390001315

48. Baroncini, M., Silvi, S., Venturi, M., & Credi, A. (2010). Reversible photoswitching of rotaxane character and interplay of thermodynamic stability and kinetic lability in a self-assembling ring-axle molecular system. *Chemistry—A European Journal, 16*, 11580–11587.

49. Casimiro, L., et al. (2018). Photochemical investigation of cyanoazobenzene derivatives as components of artificial supramolecular pumps. *Photochemical &amp; Photobiological Sciences, 17*, 734–740.

50. Yamamoto, S., Nishimura, N., & Hasegawa, S. (1971). Steric effects in azo compounds. The electric dipole moments and the absorption spectra of azobenzene derivatives. *Bulletin of the Chemical Society of Japan, 44*, 2018–2025.

51. Rau, H., & Lueddecke, E. (1982). On the rotation-inversion controversy on photoisomerization of azobenzenes. Experimental proof of inversion. *Journal of the American Chemical Society, 104*, 1616–1620.

52. Forber, C. L., Kelusky, E. C., Bunce, N. J., & Zerner, M. C. (1985). Electronic spectra of cis- and trans-azobenzenes: Consequences of ortho substitution. *Journal of the American Chemical Society, 107*, 5884–5890.

53. Tamaoki, N., Koseki, K., & Yamaoka, T. (1990). [22](4,4′) Azobenzenophane. *Angewandte Chemie International Edition, 29*, 105–106.

54. Würthner, F., & Rebek, J. (1995). Photoresponsive synthetic receptors: Binding properties and photocontrol of catalytic activity. *Journal of the Chemical Society, Perkin Transactions, 2*, 1727–1734. https://doi.org/10.1039/P29950001727

55. Lu, Y.-C., Diau, E.W.-G., & Rau, H. (2005). Femtosecond fluorescence dynamics of rotation-restricted azobenzenophanes: New evidence on the mechanism of trans → cis photoisomerization of azobenzene. *Journal of Physical Chemistry A, 109*, 2090–2099.

56. Hallett-Tapley, G. L., et al. (2013). Gold nanoparticle catalysis of the cis–trans isomerization of azobenzene. *Chemical Communications, 49*, 10073–10075.

57. Baroncini, M., Silvi, S., Venturi, M., & Credi, A. (2012). Photoactivated directionally controlled transit of a non-symmetric molecular axle through a macrocycle. *Angewandte Chemie International Edition, 51*, 4223–4226.

58. Rau, H. (1990). *Photochromism Molecules and Systems*. Elsevier.

59. Funke, U., & Grützmacher, H.-F. (1987). Dithia-diaza[n. 2] paracyclophane-enes. *Tetrahedron, 43*, 3787–3795.

60. Michl, J., Thulstrup, E. W., & Eggers, J. H. (1970). Polarization spectra in stretched polymer sheets. Physical significance of the orientation factors and determination of π-π* transition moment directions in molecules of low symmetry. *Journal of Physical Chemistry, 74*, 3878–3884.

61. Michl, J., & Thulstrup, E. W. (1987). Ultraviolet and infrared linear dichroism: Polarized light as a probe of molecular and electronic structure. *Accounts of Chemical Research, 20*, 192–199.

62. Fischer, E. (1967). Calculation of photostationary states in systems A = B when only A is known. *Journal of Physical Chemistry, 71*, 3704–3706.

63. Klan, P., & Wirz, J. (2009). Techniques and methods. *Photochemistry of Organic Compounds: From Concepts to Practice*. https://doi.org/10.1002/9781444300017.ch3

64. Stranius, K., & Börjesson, K. (2017). Determining the photoisomerization quantum yield of photoswitchable molecules in solution and in the solid state. *Science and Reports, 7*, 41145.